available at www.sciencedirect.com

SCIENCE DIRECT®

www.elsevier.com/locate/brainres

BRAIN RESEARCH

Research Report

Hemodynamic correlates of epileptiform discharges: An EEG-fMRI study of 63 patients with focal epilepsy

Afraim Salek-Haddadi[a,b], Beate Diehl[c], Khalid Hamandi[a,b], Martin Merschhemke[e], Adam Liston[a,b], Karl Friston[d], John S. Duncan[a,b], David R. Fish[a,b], Louis Lemieux[a,b,]*

[a]*Department of Clinical and Experimental Epilepsy, Institute of Neurology, Queen Square, London, UK*
[b]*MRI Unit, National Society for Epilepsy, Chalfont St Peter, Buckinghamshire, UK*
[c]*Department of Neurology, Section of Adult Epilepsy, The Cleveland Clinic Foundation, Cleveland, Ohio, USA*
[d]*Wellcome Department of Imaging Neuroscience, Institute of Neurology, Queen Square, London, UK*
[e]*Epilepsie-Zentrum Berlin am Koenigin-Elisabeth-Krankenhaus Herzberge, Herzbergstrasse 79, Berlin, Germany*

ARTICLE INFO

Article history:
Accepted 22 February 2006
Available online 5 May 2006

Keywords:
EEG
fMRI
Interictal
Spike
Epilepsy
BOLD
Localization

ABSTRACT

Using continuous EEG-correlated fMRI, we investigated the Blood Oxygen Level Dependent (BOLD) signal correlates of interictal epileptic discharges (IEDs) in 63 consecutively recruited patients with focal epilepsy. Semi-automated spike detection and advanced modeling strategies are introduced to account for different EEG event types, and to minimize false activations from uncontrolled motion. We show that: (1) significant hemodynamic correlates were detectable in over 68% of patients in whom discharges were captured and were highly, but not entirely, concordant with site(s) of presumed seizure generation where known; (2) deactivations were less concordant and may non-specifically reflect the consequential or downstream effects of IEDs on brain activity; (3) a striking pattern of retrosplenial deactivation was observed in 7 cases mainly with focal discharges; (4) the basic hemodynamic response to IEDs is physiological; (5) incorporating information about different types of IEDs, their durations and saturation effects resulted in more powerful models for the detection of fMRI correlates; (6) focal activations were more likely when there was good electroclinical localization, frequent stereotyped spikes, less head motion and less background EEG abnormality, but were also seen in patients in whom the electroclinical focus localization was uncertain. These findings provide important new information on the optimal use and interpretation of EEG-fMRI in focal epilepsy and suggest a possible role for EEG-fMRI in providing new targets for invasive EEG monitoring.

1. Introduction

The accurate spatial localization of epileptiform EEG activity remains central in both the diagnosis and treatment of the epilepsies (Fish, 2003). In patients with focal epilepsy, successful surgery relates directly to the confidence with which the 'epileptogenic zone' – theoretically defined as the minimum volume of tissue whose resection

* *Corresponding author*. MRI Unit, National Society for Epilepsy, Chalfont St Peter, Buckinghamshire, UK. Fax: +44 1494 875666.
E-mail address: l.lemieux@ion.ucl.ac.uk (L. Lemieux).

0006-8993/$ – see front matter © 2006 Elsevier B.V. All rights reserved.
doi:10.1016/j.brainres.2006.02.098

is both necessary and sufficient for seizure ablation (Luders et al., 1993) – can be identified. Despite well over a century of epilepsy surgery (Horsely, 1886), a non-invasive gold standard technique for prospectively mapping the epileptogenic zone is still lacking (Rosenow and Luders, 2001). The irritative zone, the source of interictal epileptic activity recorded on the EEG, is typically closely related to the epileptogenic zone but remains anatomically difficult to define using EEG alone (Engel, 1993; Luders et al., 1993). This is principally due to the inverse problem (Plonsey, 1963).

EEG-correlated fMRI (EEG-fMRI) can be used to map Blood Oxygen Level Dependent (BOLD) signal changes linked to spontaneous EEG activity non-invasively and has attracted a great deal of interest as both a scientific and clinical tool (Salek-Haddadi et al., 2003; Schomer et al., 2000). A number of groups have previously reported BOLD activations in relation to IEDs using a variety of methods (Al Asmi et al., 2003; Jager et al., 2002; Krakow et al., 2001a, 1999; Lazeyras et al., 2000; Patel et al., 1999; Seeck et al., 1998; Symms et al., 1999; Warach et al., 1996). Consensus however is still lacking on several key issues such as which EEG characteristics lend themselves best to EEG/fMRI? What comprises a biologically meaningful activation? What is the range of BOLD responses to IEDs? What influences these responses and how these can be best modeled and characterized experimentally? How should any anatomical information be used clinically? What is clear is that these studies remain difficult to perform for several reasons. Firstly, patient selection, generally based on a high rate of stereotyped IEDs, is limiting. IEDs themselves may be sparse and difficult to discern. Secondly, by nature, studies of spontaneous EEG activity are not as powerful or efficient as studies allowing experimental manipulations via a paradigm. This may explain why only half of experiments in patients with focal epilepsy and in whom IEDs are recorded tend to yield significant activations; thirdly, there is little consensus or comparison on how data should be analyzed. The available data do however suggest that there is good test–retest reproducibility where activations are observed and most, but by no means all, positive cases show at least one activation concordant with conventional localization.

Using continuous EEG-fMRI, we aimed to establish the range of activation patterns linked to IEDs across different epilepsy syndromes and pathologies; to evaluate the relative proportion of focal epilepsy patients showing BOLD activations using EEG/fMRI; to explore the clinical

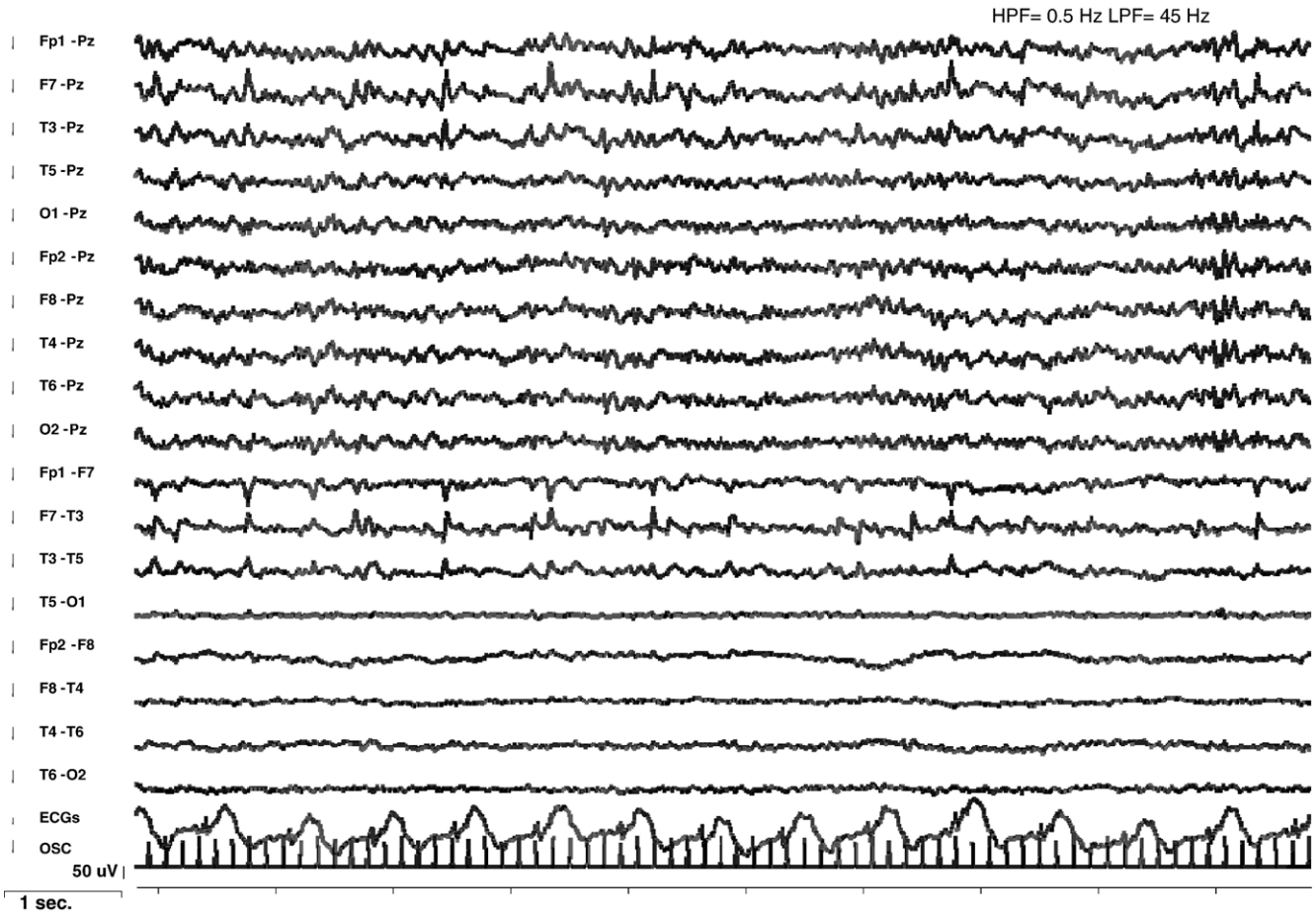

Fig. 1 – EEG recorded during fMRI from patient #25 showing left anterior temporal spikes. Pulse and imaging artefact have been removed. Two bi-temporal chains are shown, referenced to Pz in the top ten channels, followed by a bipolar montage in the next eight. ECG and slice timing signals (OSC) are shown at the bottom.

Table 1 – Electroclinical data

Case	Onset age (year)	Aetiology	Seizure type	Structural MRI	Ictal EEG	Interictal EEG	Localization
1	0	Post left temporal lobectomy for DNET, plus R-HS	CPS, SGTCS	Extensive left temporal lobectomy with considerable amount of altered brain surrounding cavity.	Subdural electrodes: Left frontal or possibly contralateral seizure onset, outside of the resected areas	Intermittent and widespread theta. Frequent temporal sharp waves and spikes with shifting lateralization, predominantly left mid temporal.	Uncertain
2	7	MCD	FMS	Diffuse cortical thickening right hemisphere, within parietal and occipital lobes, extending to frontal region.	Right temporal spikes	Widespread, right-sided spikes, sharp waves, and sharp and slow waves maximal frontocentral and centrotemporally.	R Lateralized
3	7	MCD	CPS, SGTCS	Widespread band and subcortical nodular heterotopia, predominantly posterior.	No clear changes	Bilateral, posterior temporal/occipital sharp and slow wave complexes with some left-sided spikes.	Bilateral
4	3	DNET	CPS, SGTCS (non-localizing/ lateralizing)	Focal lesion expanding left middle temporal gyrus. Left temporal lobe is smaller than the right.	No clear lateralization	Left-sided slowing, bursts of bilateral spike and wave/ polyspikes, left temporal spikes.	Diffuse
5	0	MCD	CPS, SGTCS	Extensive MCD involving both hemispheres.	–	Left-sided spikes, sharp waves and slow waves, some bilaterally synchronous and occasionally right-sided.	Diffuse
6	40	Chronic encephalitis	FMS, CPS, SGTCS	Mild atrophy of left cerebral hemisphere.	Widespread over left hemisphere	Left midtemporal spikes and slow waves.	L Cent-Temp
7	15	Low-grade astrocytoma (post surgery and radiotherapy)	SPS, CPS	Focal scarring of left middle frontal gyrus.	Widespread over left hemisphere	Left frontal spikes.	L Front
8	5	Post-traumatic	SGTCS	MRI negative	–	Left temporal slowing with frequent left anterior temporal spikes.	L Lateralized
9	1	L-HS	SPS, CPS	Severe diffuse L-HS	No lateralization	Left anterior temporal spikes.	L Temp
10	4	L-HS	CPS, SGTCS	L-HS	Left lateralization	Bursts of left-sided frontotemporal spikes. Sometimes occurring bilaterally.	L Lateralized
11	0	Perinatal subarachnoid haemorrhage	CPS, SGTCS	Left cystic encephalomalacia plus L-HS	–	Left-sided slowing with left posterior temporal spikes.	L Lateralized
12	1	Unknown (Family history, post-vaccine seizures, and L-HS);	MJ, SPS, CPS, SGTCS	L-HS	No lateralization	Left anterior temporal spikes and sharp waves.	L Temp
13	18	L-HS	CPS	L-HS	Left hemisphere	Left temporal slow and sharp waves.	L Temp
14	3	Cryptogenic	SPS, CPS, SGTCS	MRI negative	No clear lateralization	Bifrontal spike-wave discharges with right-sided emphasis.	Uncertain
15	5	Cryptogenic Occipital lobe epilepsy	SPS (Visual phenomena R ≫ L)	MRI negative	–	Left posterior temporal/ occipital spikes and sharp waves.	L Occ/Temp
16	5	Cryptogenic	CPS (frontal semiology), SGTCS	MRI negative	–	Spikes over right hemisphere with wide field, maximal temporally.	Uncertain

Table 1 (*continued*)

Case	Onset age (year)	Aetiology	Seizure type	Structural MRI	Ictal EEG	Interictal EEG	Localization
17	3	Grade II left parietal astrocytoma resected at age 11	SPS, SGTCS	Large temporoparietal resection.	Widespread over left hemisphere	Left posterior temporo-parietal spikes.	L Lateralized
18	19	Cryptogenic	CPS, SGTCS	MRI negative	Multifocal onset	Left temporal slow waves and spikes plus right temporal spikes during sleep.	Diffuse
19	7	Cryptogenic	CPS (extra-temporal semiology), SGTCS	MRI negative	Bilateral onset	Left temporal sharp waves and spikes with bilateral frontal sharp waves.	Uncertain
20	3	HS	CPS, SGTCS	L-HS	Widespread over left hemisphere	Spikes and sharp waves intermixed with slow activity over left anterior to mid temporal regions.	L Lateralized
21	4	MCD	SPS, FMS, SGTCS.	Right parietal open leptoschizencephaly.	–	Bursts of spike-wave activity over central region bilaterally.	R Frontal
22	5	DNET	SPS, SGTCS	Right temporal lobe lesion involving amygdale and uncus but not hippocampus.	No clear lateralization [a]	Right-sided anterior temporal spikes with some independent left-sided spikes.	Diffuse
23	9	Post-traumatic	CPS, SGTCS	Right middle frontal gyrus cortical scar.	–	Right-sided polyspike and slow wave discharges, single and in bursts, maximal centro-temporally.	R Frontal
25	1	Neoplasm	CPS, SGTCS	Mass in left temporal lobe involving amygdala, hippocampus and parahippocampal gyrus associated with irregular cystic cavity.	No clear change	Left anterior temporal spikes.	L Temp
26	4	FCD	CPS, SGTCS	Focal signal change in left middle frontal gyrus consistent with focal cortical dysplasia.	–	Independent left and right mid-temporal spikes and slow-waves. L >> R.	Uncertain [b]
27	7	MCD	CPS, SGTCS	Marked malformation affecting both hemispheres, mainly the right. The right hemisphere is smaller and the fronto parietal regions are most affected.	–	Spikes, sharp-waves, and slow-waves widespread over the right.	R Lateralized
29	3	MCD	SPS (simple visual hallucinations)	Extensive MCD affecting the left cerebral hemisphere, particularly the posterior part. Does not affect the frontal lobe.	–	Bilaterally synchronous spikes over occipital and posterior temporal areas.	L Occ
30	8	Cryptogenic	CPS, SGTCS	MRI negative	Widespread over left hemisphere	L fronto-temporal bursts of spikes, sharp waves, and spike and slow-waves.	L Lateralized
31	0	MCD	SPS, CPS, SGTCS	Two large heterotopic nodules: Frontoparietocentral and medial parietal.	–	Frequent right centro-parietal spikes.	R Frontoparietal
35	<10	MCD	SPS, CPS, SGTCS	Left hemisphere atrophy with parietal polymicrogyria and L-HS.	Widespread over left hemisphere	Left anterior-mid temporal spikes.	L Lateralized

(continued on next page)

Table 1 (*continued*)

Case	Onset age (year)	Aetiology	Seizure type	Structural MRI	Ictal EEG	Interictal EEG	Localization
36	3	FCD	SPS	Thickened cortex in the left antero-inferior parietal region just extending into the inferior frontal gyrus.	No change	Continuous Left parietal spikes.	L Parietal
37	14	L-HS	CPS (temporal semiology)	Severe diffuse L-HS.	Independent right and left seizure onsets with temporal lobe-type automatisms. Psychometry non-lateralizing.	Left anterior-mid temporal spikes and slow waves.	Temp, uncertain laterality.
38	5	Cryptogenic	CPS, SGTCS	MRI negative	–	Right-sided mid-anterior temporal sharp waves plus rare independent left-sided sharp waves.	Diffuse
39	7	L-HS	CPS, SGTCS	L-HS	Left temporal onset	Left anterior temporal spikes.	L Temp

Abbreviations: Bil = Bilateral; CPS = Complex partial seizure; DNET = Dysembryoplastic neuroepithelial tumor; FCD = Focal cortical dysplasia; FMS = Focal Motor Seizures; HS = Hippocampal sclerosis; MCD = Malformation of cortical development; MJ = Myoclonic jerk; Post = Posterior; SGTCS = Secondary generalized tonic–clonic seizure; SPS = Simple partial seizure.

[a] #22: Two distinct seizure types were recorded during video telemetry. One type would begin with a peculiar feeling around the head, followed by head slumping to the right, unresponsiveness and post-ictal dysphasia lasting minutes. Here, ictal changes were seen bilaterally but greater on the left. The second type began with the same aura followed by clasping together of the hands, rocking movements of the arms, followed by fidgeting and secondary generalization into a tonic–clonic seizure. This attack began with right fronto-temporal fast activity.

[b] #26: Frontal lesion, seizure semiology non-localizing and non-lateralizing, bi-temporal spiking, no ictal recording.

relevance of any fMRI findings; and to identify patients for whom the technique holds greatest promise. Our primary focus was on mapping IEDs and to this end, our study included both patients with and without electroclinically well-defined epileptogenic foci in the hope that information obtained with regards to anatomical concordance between the fMRI activation and the epileptogenic focus in the former, would in turn help validate fMRI findings in the latter group. We also aimed to characterize the hemodynamic responses to focal IEDs specifically in this group to avoid doubts as to the biological significance of the areas interrogated.

Methodologically, we aimed to explore different ways of maximizing information from the EEG (both manual and semi-automated), of minimizing the deleterious effects of patient head motion, and of constructing better models of the EEG data for fMRI analysis. In particular, we used statistical tests to elucidate the importance of modeling runs of IEDs compared to individual events, and of taking into account non-linearity in the BOLD response in cases with very frequent discharges. The results provide guidance on the best analytical strategy for IED-correlated fMRI data. Finally, we aimed to identify qualitatively and retrospectively, any experimental factors linked to the likelihood of activation.

2. Results

Four of the 63 patients who underwent EEG-fMRI were excluded from further analysis: one due to the presence of post-operative MR artefacts, 2 due to excessive head motion that rendered the EPI data un-interpretable and in one, the scan was terminated because of a spontaneous convulsive seizure.

None of the patients reported any discomfort or adverse effects from EEG-fMRI, and EEG quality readily allowed the identification of IEDs (Fig. 1). In 25 patients (42%), no IEDs were observed. These patients were not clinically distinguishable from those in whom IEDs were captured. One patient was studied on three occasions with a sub-clinical electrographic seizure recorded during one of these and was presented elsewhere (Salek-Haddadi et al., 2002). Repeat data were acquired in 5 cases in which IEDs were captured (#7, #23, #25, #27 and #38).

We recorded IEDs in 34 patients (16 males, mean age 32 years, range 20–63) the clinical details of whom are provided in Table 1. The mean number of events captured during each 35-min recording session was 286 (range = 12–1710, median = 103). 25 patients had 1 event type only, 7 had 2 event types and 2 had 3 event types (Table 2 and Web Table 1).

The overall findings in terms of yield, sign and concordance of the significant BOLD activations are summarized in Fig. 2. In Figs. 3–5 we present more detailed results from 3 patients to illustrate different types of activation patterns, degrees of concordance and diagnoses. All other results are provided as supplementary data (Web Figs. 1–20).

2.1. *fMRI activation and concordance*

The clinical fMRI results for all patients, in whom IEDs were captured, are presented in Table 2. The full description of

the fMRI models and result statistics are provided in Web Table 1. In summary, 10 of 34 patients (29%) had significant positive BOLD changes only, 4 (12%) had negative changes only, 9 (26%) patients had both and 11 (32%) had no significant change. The mean number of discharges observed per experiment in cases with significant activation or deactivation was 355, and 148 for the cases with no activation or deactivation. The lowest number of discharges recorded in a case where activation or deactivation was revealed was 12 (case #15) but the activation was tiny (1 suprathreshold voxel only). The highest number of discharges captured in a case with no activation was 971 (case #20).

Significant IED-linked BOLD changes were seen in 23 of the 34 patients with discharges during fMRI acquisition. Considering positive and negative BOLD changes together, where available, there was concordance with electro-clinical data in 17 patients, comprising 7 *Concordant* and 10 *Concordant Plus*, *Discordant* in 2 patients and *Nil* findings in 5. Activations were *Concordant* in 10 patients, *Concordant Plus* in 5, *Discordant* in 2. Deactivations were *Concordant* in 1 patient, *Concordant Plus* in 2 patients, and *Discordant* in 7. In the ten remaining patients with diffuse or uncertain localization, 4 had significant BOLD changes, 2 positive and 2 negative (see Web Figs. 1,4, 12 and 18).

In terms of aetiology, 4 of the 8 MCD cases were concordant, (3 *Concordant*, 1 *Concordant Plus*) and 4 had *Nil* findings. Only 1 of the MCD cases showed significant deactivation (*Concordant Plus*). For pure HS, the findings were 2 *Concordant*, 1 *Concordant Plus*, 1 *Discordant*, and 2 *Nil*. The deactivation findings were 1 *Concordant Plus*, 3 *Discordant* and 2 *Nil*.

The maximum deactivation was remote from the concordant activation in all cases except #12. For example, deactivations were found in the central structures or retrosplenial (including bilateral medial occipital) in 8 cases (5 with lateralized or focal activations, 1 with midline activation (#7) and 2 without activation (#29 and #18)).

Of the five patients with no activation and a localized/lateralized seizure focus (#17, #20, #21, #27, #30), two (#17 and #30) showed few scattered specs on uncorrected SPMs but the others nothing. In these cases, analysis using a flexible set of basis functions also failed to reveal any concordant foci. In #17 there was a single voxel in the brainstem, In #20, event onsets were automatically detected. There were scattered voxels throughout but no concordant foci. In #21 and #27, there was nothing and in #30, there was a very small right frontal cluster of uncertain significance.

2.2. The hemodynamic response to IEDs

The results for each case are listed in Web Table 2. In summary, the mean peak amplitude for activations ($N = 15$) was 0.46% (range: 0.07–1.70) and −0.52% for deactivations ($N = 2$; −0.16 and −0.88). The mean time to peak was 5.3 s (range: 2.5–9.5 s) and the mean time to undershoot 21.2 s (range: 10.5–31.5 s) for the positive responses, and mean time to (negative) peak 9 s (6.5–11.5) and overshoot 24 s (range: 21.5–26.5 s) for negative responses. The mean undershoot to peak ratio was 0.54 (range: 0.02–1.21) for the positive responses and the mean overshoot to negative peak ratio was 0.91 (range: 0.88–0.94) for the negative responses.

2.3. IED characteristics and the BOLD response

2.3.1. Cases with multiple IED types

Of the four cases with multiple IED types, the distinction was in terms of IED amplitude in 3 (#6, #31, #35), and field distribution in the other (#25). In summary: in patient #6, the smaller IEDs contributed very little to the activation such that failing to distinguish between the events would be detrimental to sensitivity. In case #25a, we were able to demonstrate a statistically significant difference in activation linked to the F7 versus T3 spikes with a relatively greater contribution of the former to the anterior segments of the activation in the first session. In the second session (#25b), this difference could not be seen. In case #31, the largest responses were linked to the large spikes followed in order by the smaller spikes and finally the slow waves but the difference in response was not statistically significant enough to warrant accounting for within the model. In case #35, there was a statistically significant difference between responses to the three event types (see Web Table 1 for detailed results).

2.3.2. Cases with runs of IEDs

In case #3, there was no significant effect over the additional regressors, indicating that event duration was not a factor. In #7a, #13, #23a and #23b, however, a significant proportion of variance was attributable to event duration (see Fig. 4). Interestingly, in #13, there was retrosplenial deactivation in addition with the more complex model (see Fig. 3).

2.3.3. Cases with very frequent IEDs

Significant non-linear effects were demonstrated in #6, #7b, #8, #9, #12, #39, but not #31 and #11. Notably, in #6, #7, #8, #12 and #39 the second-order Volterra kernels were negative indicating a saturation effect of the BOLD response to frequent events. In case #9, non-linear positive effects were observed most significantly within the ipsilateral cluster but also within the contralateral cluster.

2.4. Factors influencing activation

On average, all motion parameters were larger in the no-BOLD cases with the difference reaching statistical significance for the mean scan-to-scan displacement, $|d'|$. The mean number of spikes was larger in the BOLD group but this did not reach significance. However, cases with runs of IEDs were significantly over-represented compared to cases with individual IEDs. Abnormalities in the background EEG were also a significant factor for activation. The results of these analyses are shown in Table 3.

3. Discussion

The application of continuous EEG-correlated fMRI in focal epilepsy has allowed us to show a wide range of activation

Table 2 – fMRI results for basic model

Case	Description of IED types	fMRI Maximum		Clinical localization	Activation				Deactivation				Figure #
		Activation	Deactivation		C	C+	D	Ø	C	C+	D	Ø	
1	L Temp IED		R Front	Uncertain				•			•		W1
2	R Temp IED	R Front + R Par + L Occ		R Lateralized		•						•	W2
3	Runs of Bil Post-Temp/ Occ IED	L Post + R Post		Bilateral	•							•	W3
4	Bursts of Bil (R > L) polyspikes	L Front/Par + Bil Occ		Diffuse		•						•	W4
5	Frequent Bil synchronous spikes			Diffuse				•				•	
6	L Temp IED <250 μV L Temp IED >250 μV	L Temp	L Temp/Par	L Cent-Temp	•						•		W5
7a	Runs of bifrontal IED	Bil Mid Front + Bil Front	R Temp + Mid Occ + Bil Par	L Front		•					•		W6
7b	Bifrontal IED	Bil Mid Front + Bil Front + Bil Occ	Mid Occ + Bil Par										
8	L Temp IED R Temp IED	L Temp + more widespread and some contralat	Bil Mid Occ/Par	L Lateralized		•					•		W7
9	L Temp IED	L Temp	R Temp + L Temp + Cereb	L Temp	•						•		W8
10	Bil spike-wave	Cereb + Widespread	Occ	L Lateralized			•				•		W9
11	L Post Temp IED	L Temp		L Lateralized	•							•	W10
12	L Ant Temp IED	L Temp	L Temp + Mid Occ + R Temp + Bil Par	L Temp	•					•			W11
13	Runs of L Ant Temp IED	L Temp		L Temp	•							•	3
14	Runs of R Front generalized spike-wave	R Front + R Par		Uncertain		•						•	W12
15	L Post Temp/ Occ IED	L Occ		L Occ/Temp	•							•	W13
16	L Temp IED R Temp IED			Uncertain				•				•	
17	L Temp IED			L Lateralized				•				•	
18	Runs of L Temp IED		Mid Occ + Mid Par + Mid Front	Diffuse				•		•			W14
19	L-sided IED			Uncertain				•				•	
20	L Temp IED (Auto)			L Lateralized				•				•	
21	R-sided IED			R Frontal				•				•	
22	R Ant Temp IED			Diffuse				•				•	
23a	Runs of Bil polyspike-wave	R Front + R Par + L Cereb + R Temp	Bilat Par + Bil Occ + L Front	R Frontal		•					•		4
23b	Runs of Bil polyspike-wave	R Front + R Par + L Cereb + R Temp	Bilat Par + Bil Occ										
25a	L Front-temp IED L Temp IED	L Temp	Mid Occ	L Temp	•						•		5
25b	L Front-temp IED (Auto) L Temp IED	L Temp	Mid-frontal + Mid Occ/Par + L Front										
26	R-sided IED L-sided IED			Uncertain				•				•	
27a	R Temp IED			R Lateralized				•				•	
27b	R Temp IED												
29	L Occ IED (Auto)		L Occ + L Par + Bil Front	L Occ				•		•			W15
30	L-sided IED			L Lateralized				•				•	
31	R Cent IED <160 μV	R Front/Par		R Frontoparietal	•							•	W16

Table 2 (*continued*)

Case	Description of IED types	fMRI Maximum		Clinical localization	Activation				Deactivation				Figure #
		Activation	Deactivation		C	C+	D	Ø	C	C+	D	Ø	
	R Cent IED >160 μV R Cent slow												
35	L Front-temp spike <50 μV L Front-temp spike 50–100 μV L Front-temp spike >100 μV	L Temp		L Lateralized	•							•	W17
36	L Cent spike (Auto)	Mid Front		L Parietal			•					•	W18
37	L Temp spike		L Temp + R Temp	Temp, uncertain laterality				•		•			W19
38a	L-sided IED			Diffuse				•				•	
38b	R-sided IED												
39	L Front-temp spike (Auto)	L Temp + Bil Occ + Bil Par	R Cereb + L Cereb	L Temp		•					•		W20

Legend: IED = Interictal epileptiform discharge; Auto = automated event detection; Temp = temporal; Par = parietal; Occ = occipital; Front = frontal; Cereb = cerebellum; R = right; L = left; Bil = bilateral; Mid = midline; C = concordant; C+ = concordant plus; D = discordant; Ø = nil.

patterns linked to IEDs and address a number of important questions on the relationship between the characteristics of the EEG record and regional hemodynamic changes. Our approach is based on a novel modeling framework capable of accounting for various important EEG features and minimizing the impact of undesirable effects such as motion.

3.1. *Methodological aspects*

3.1.1. *Choice of subjects and EEG recording*

We chose to study a wide range of subjects from the outset, motivated by the need to establish the full range of fMRI correlates for interictal EEG events, irrespective of pathology. Our patient population was heterogenous providing a good base from which to explore methodological issues but with less scope for clinicopathological correlation. The choice of fMRI acquisition sequence was motivated primarily by the desire to obtain whole brain coverage with good SNR and hence investigate IED-related changes throughout the brain. Whilst the benefits of recording a greater number of EEG channels are obvious,

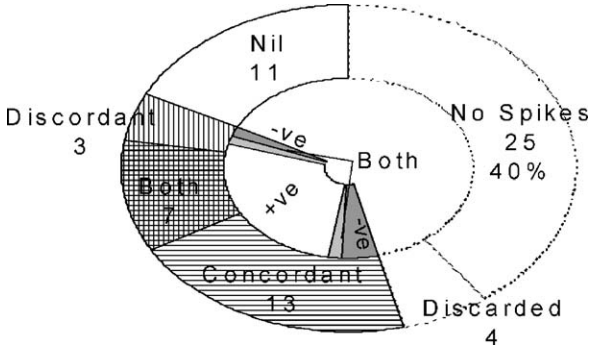

Fig. 2 – Summary of scanning and activation findings for basic model.

EEG here was used primarily for spike detection where localization was already known. The simultaneous use of high-density EEG could allow for more in depth studies of individual events or classes of events, as well as dipole modeling, all of which are the subject of ongoing efforts (Liston et al., in press-b).

3.1.2. *EEG classification and automatic spike detection*

The manual interrogation of EEG data (EEG coding) is perhaps the most crucial part of analyzing continuously-acquired EEG-fMRI data. For the purposes of modeling the entire fMRI time-series fully, one would need to account for every possible event or feature that may influence the BOLD response of the voxels under investigation. Our strategy was therefore to 'over-code' the EEG both in terms of the number of events that may be epileptiform in origin and the sub-grouping of events so that the most information was extracted from each recording. We used a consensus of opinion. This is an important step up from how EEG information was used in spike-triggered fMRI studies, whereby scanning was restricted to events with pre-determined features (Krakow et al., 1999).

We were able to show the benefits of using automated event detection to identify IEDs where visual assessment was technically difficult due to large numbers of IED. For example, in case #25 we demonstrate the activations derived using automated event detection compare extremely well with those derived conventionally from a separate session. In patients #29 and #39, we were able to demonstrate concordant BOLD changes using this method also, but not in #20. This may reflect differences in paradigm efficiency or 'loss of baseline' (see (Salek-Haddadi et al., 2003) for further discussion). To our knowledge, automatic event detection has never been applied to EEG-fMRI.

3.1.3. *Motion and modeling implications*

Due to the noisy nature of the fMRI signal, the ability to infer effects rests on careful hypothesis testing. Devising

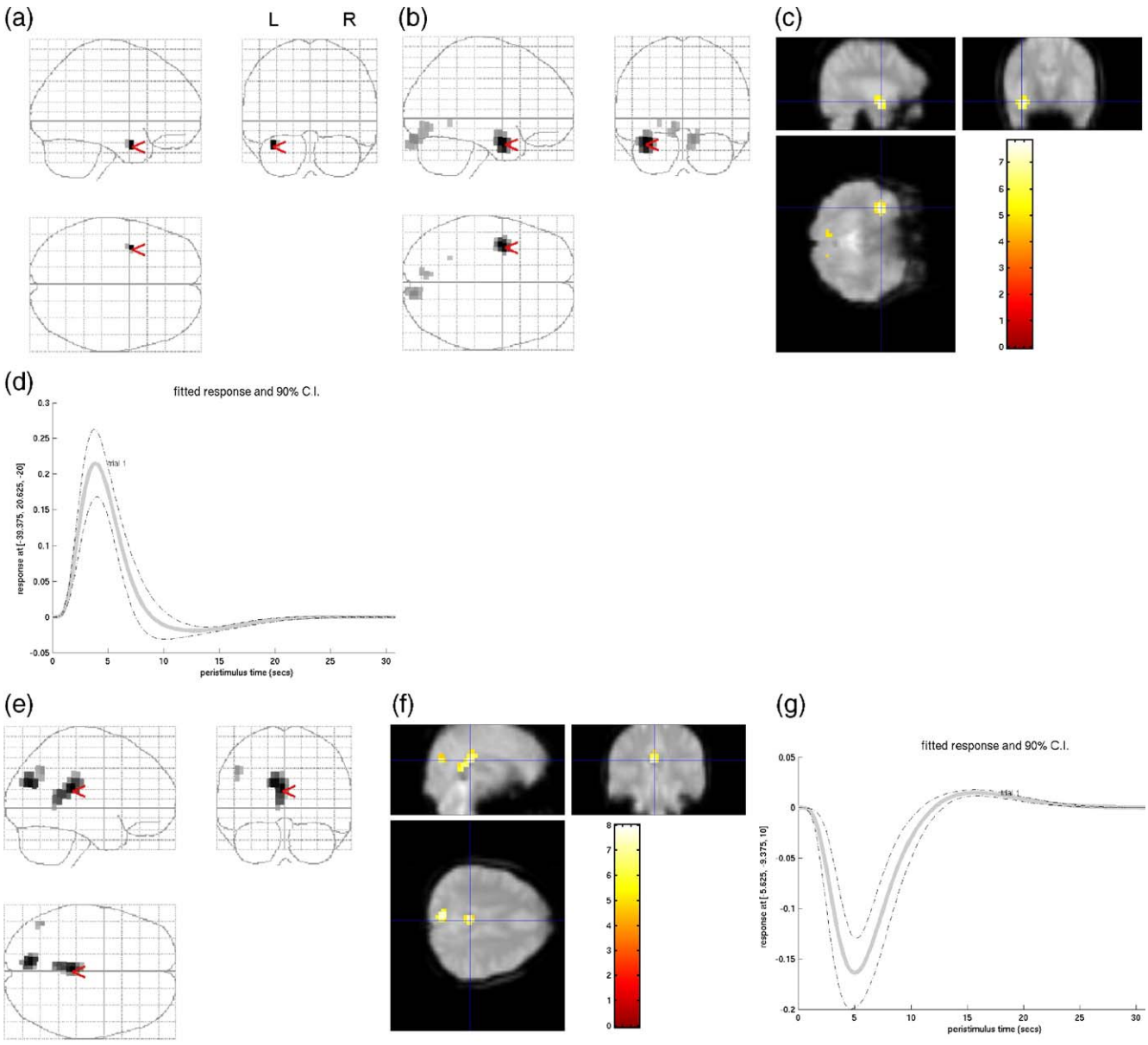

Fig. 3 – Concordant activation and Discordant deactivation: effect of event duration. Patient #13 had left hippocampal sclerosis and left-temporal IEDs. EEG/fMRI revealed a highly concordant cluster of left temporal activation (overall maximum indicated by red arrow in glass brain and cross-hair on EPI) with smaller clusters in the occipital region (a); more pronounced when discharge duration was taken into account (b); EPI overlay and hemodynamic response shown in panels c and d, respectively. Incorporating duration into the model also resulted in a retrosplenial deactivation pattern, shown in panels e, f, with the fitted hemodynamic response in panel g. (For interpretation of the references to colour in this figure legend, the reader is referred to the web version of this article.)

realistic models based on the EEG events of interest is therefore crucial and remains one of the technique's main challenges. Our results show that the IED-related BOLD responses could be captured effectively using the canonical HRF (plus its time derivative). Previously, the application of the Fourier expansion set allowed us to confirm the physiological nature of concordant IED-related BOLD responses in specific cases (Diehl et al., 2003; Lemieux et al., 2001). In the patients studied here, this more flexible modeling approach resulted in no increase of concordant activations. This suggests that the approach adopted, based on the canonical HRF (plus time-derivative), was sufficiently capable of capturing the variability in BOLD response but there are several intermediate strategies for example, the sequential application of multiple HRFs followed by correction for multiple tests (Bagshaw et al., 2004). The optimal choice of basis function remains an empirical question; however, higher degrees of modeling flexibility generally translate into lower sensitivity and specificity. We note that increasing the number of samples could

increase the yield with a more flexible basis set but our results suggest that this increase would be greater for a reduced set such as the one used in this work.

Bagshaw et al. (2005) suggested that event duration should be considered when modeling IED-related BOLD. They looked at the effect of IED duration on the positive BOLD response in selected mixture of patients with both idiopathic generalized and focal epilepsy but did not statistically assess the significance of any extra contribution. We were able to demonstrate that significantly improved models could be obtained by accounting for different EEG event topographies and durations. For example, the results for case #6 demonstrate that failing to distinguish between the two event types within the model would reduce sensitivity since the small spikes do not contribute significantly to the activation. For runs of IEDs, we were able to demonstrate significantly improved models in three cases. Together, these findings show that in cases with different types of IED, a decision ought to be made concerning whether or not the different types are likely to share the same anatomical generators. Where this is not the case then separate regressors ought to be used and tested individually. In cases where different types of IED are presumed to share a unique generator nested models should be used to determine the best strategy. Moreover, consideration ought to be given to including both duration and saturation effects in the modeling in cases featuring runs or very frequent IED, with significant effects demonstrated in some cases in our series.

Motion remains an important concern in the analysis of fMRI data, even with the best immobilization measures (Lund et al., 2005) and particularly in patient populations. In cases where the motion bears no relationship to the experimental variables (i.e., non-stimulus correlated) activations linked to the effects of interest may be 'drowned out' by the consequent increase in noise. However, in cases where the head motion is stimulus correlated (i.e., coincident with events of interest), the result can be artefactual areas of false activation or a decrease in specificity. The effects are complex and unpredictable and we do not feel that this point has received due consideration in the epilepsy literature so far (Salek-Haddadi et al., 2003). We address this by incorporating motion into the fMRI model, reducing the likelihood that any given activation is the result of motion alone, partly trading sensitivity for specificity. Whilst previously necessary to PET, the use of global signal covariates or global scaling in fMRI carries well-recognized problems (Aguirre et al., 1998a), most pertinently in relation to the interpretation of deactivations. For this reason, we have avoided doing so. Furthermore, head motion can also give rise region-specific/boundary effects. There was no visible correlation between the EEG events and head motion in the data presented here.

3.1.4. *The assessment of concordance*

There are two important choices that have to be made in assessing concordance, the first is what to judge against and the second is how. Like previous studies, we chose to assess concordance by comparing EEG/fMRI against the best available indicators to the epileptogenic zone. The inclusion of patients with diffuse or uncertain electroclinical localization was motivated by the need to study more patients in order to test the technique at a time when no other continuous EEG/fMRI studies were available. Both ourselves (Lemieux et al., 2001) and others however have since established some basic principles (Al Asmi et al., 2003; Bagshaw et al., 2004; Benar et al., 2002). Despite the lack of surgical data in our series, we avoided judging fMRI localization against scalp EEG alone as we felt this would be of less clinical interest and prevent comparison with other EEG/fMRI studies.[1] How to judge concordance is not a new problem in EEG/fMRI (Salek-Haddadi et al., 2003).

fMRI maps generally contain multiple activations that are strongly threshold dependent. In contrast to other, even more recent studies (Federico et al., 2005; Kobayashi et al., 2005), we have chosen to use a conventional and fixed thresholding method across the board to avoid bias and facilitate comparison. There are obvious difficulties in translating imagery as complex as fMRI maps into words and lobes especially given that neither fMRI activations nor pathological lesions respect the traditional anatomical boundaries between lobes or quadrants. This is however necessary to compare against 'electroclinical localization' as derived from a range of different sources. The distinction between *Concordant* and *Concordant Plus* is also important in that more distant or diffuse activations are either indicative of remote effects or represent false positive activations (e.g., stimulus correlated motion) both of which are important to recognize. Several previous studies have potentially ignored such effects, reporting only on activation within a region of interest (Archer et al., 2003) or lesion (Kobayashi et al., 2005). We feel the full reporting of activations in their entirety is important and should be encouraged (Salek-Haddadi et al., 2003).

3.2. *Clinical and neurobiological aspects*

3.2.1. *Yield, localization and clinical relevance*

Overall, BOLD changes were revealed in 67% of patients in whom IEDs were detected during scanning and this is in line with previous studies (Al Asmi et al., 2003; Krakow et al., 2001b). There was a tendency for more spikes, less motion, more runs of IEDs and less EEG background abnormality in cases with activation, which has not been shown before. A similar analysis for the negative responses revealed that the BOLD cases had three times the number of events as the non-BOLD cases ($P<0.011$) and a significantly lower degree of

[1] Doing so, however, would not alter the results significantly. This is because in two cases (#7 and #23) IEDs recorded inside the scanner (and the subsequent activations) were bilateral, whereas IEDs previously recorded outside were unilateral and in #37 (Concordant Plus deactivation) there is bilateral deactivation to left temporal IEDs in the context of a temporal lobe focus of uncertain laterality These cases are hence Concordant Plus whatever and in cases #1, #4 and #18 concordance with EEG alone is still negative.

head motion. The activation/deactivation patterns were mostly diffuse, involving more than one lobe. Reproducibility, assessed in five cases was good, and included two cases with no activation on both occasions. The relationship between extent of EEG abnormality and fMRI activation pattern was varied, bilateral activation patterns being sometimes linked to bilateral IEDs (e.g., cases #3 and #7), while in some cases, unilateral cerebral activations were found with bilateral IEDs (e.g., #23, Fig. 4, and #14) and vice versa (#2, #37, #39).

All but two patients with localized/lateralized or bifocal electroclinical findings in whom there was activation showed some degree of concordance (#10, #36). The BOLD changes were often much more extensive than expected

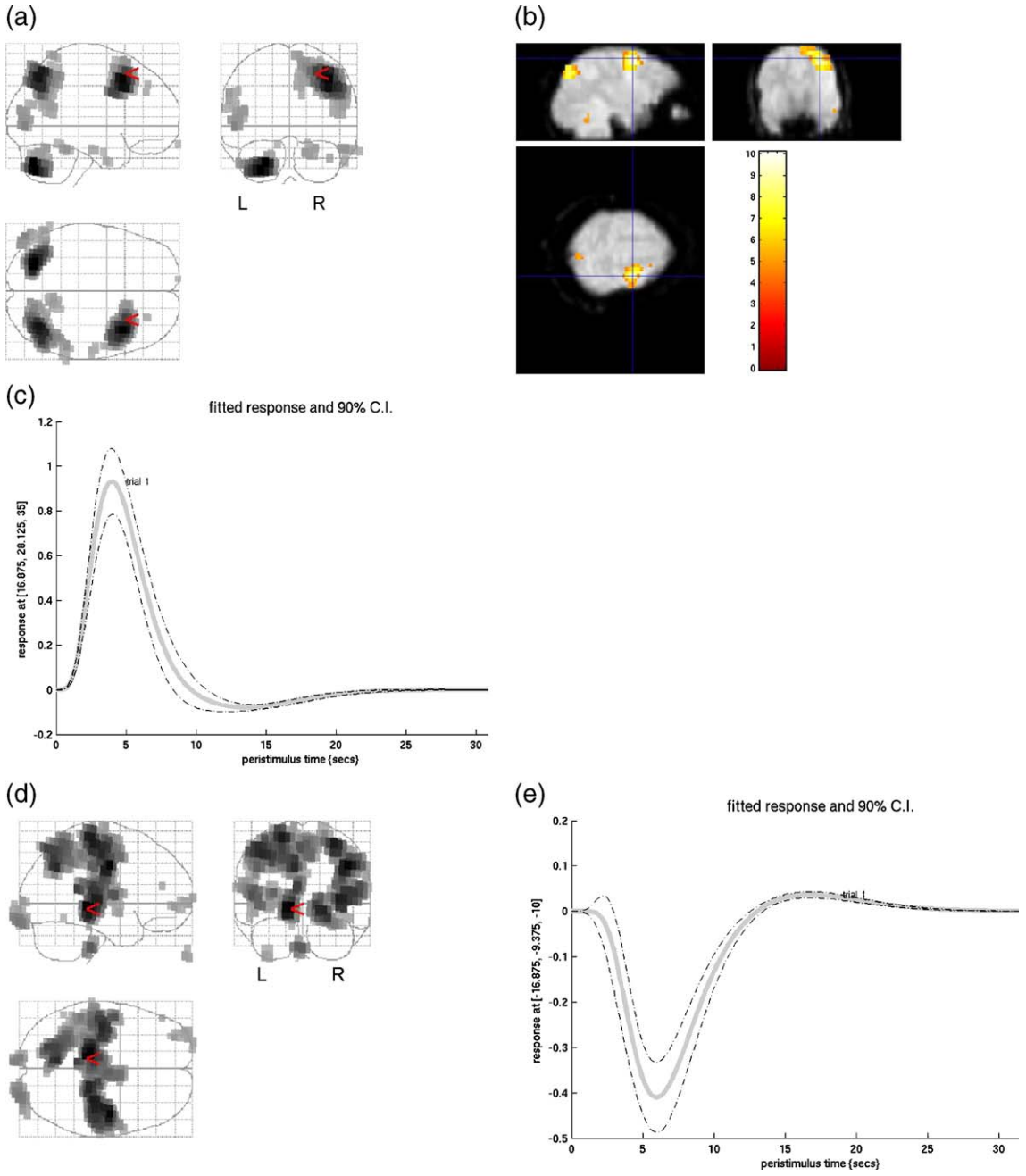

Fig. 4 – Concordant Plus activation/Discordant deactivation: Patient #23 had a post-traumatic right middle frontal gyrus scar. At the age of 8, the patient suffered a head injury, and developed secondary generalized tonic–clonic seizures and partial seizures, beginning with head/eye deviation to the left. In 2 separate EEG-fMRI sessions, runs of polyspike-wave activity were captured (198 and 236 in each session, respectively) and mapped to three distinct clusters with excellent reproducibility. A diffuse pattern of activation with a concordant maximum from the first session is shown in panel a, overlaid onto the mean EPI in panel b, with hemodynamic response shown in panel c. There were also areas of deactivation (d) with the signal change shown in panel e. The same results are also shown for the second session in panels f–i.

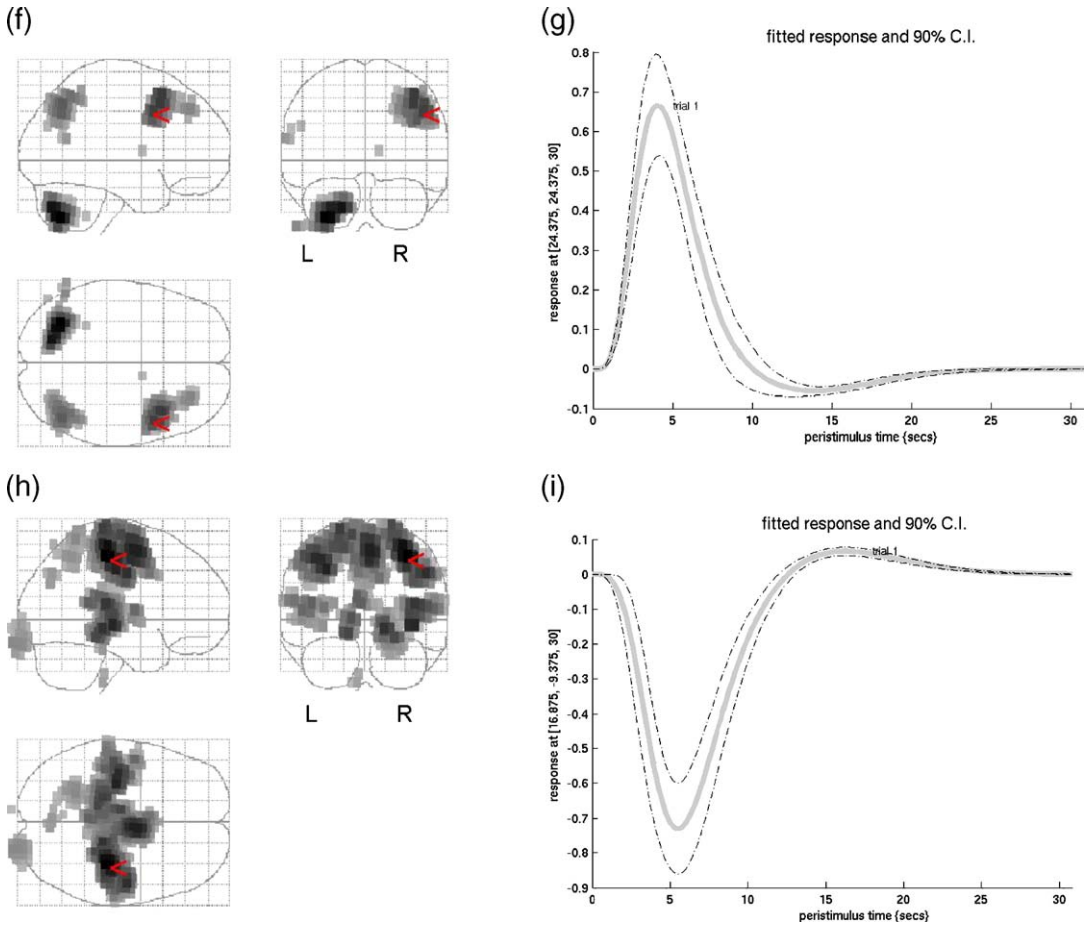

Fig. 4 *(continued).*

from the focal nature of the electroclinical findings, and often included discordant areas. This is similar to the findings from other functional interictal studies in partial epilepsy such as 18FDG PET, which typically reveal much larger areas of metabolic change than the epileptogenic zone, possibly reflecting areas of functional deficit (see Mauguiere and Ryvlin, 2004).

Temporal spikes generally resulted in concordant (lateral) activations with the single discordant finding linked with bilateral fronto-central spikes. Deactivations were common in temporal lobe epilepsy, and often remote. The general picture for activations in MCD is very similar to that in TLE, with good concordance and activations often localized within the structural abnormality (e.g., case #2).

In general, positive changes tended to be highly concordant at least for the lobe of presumed seizure localization, while negative changes appeared to be much less in agreement with the electroclinical findings and were more critically dependent on the number of IEDs, possibly reflecting a smaller or more variable effect for individual IEDs compared to the positive BOLD changes. A pattern of deactivation in the retrosplenial region (precuneus and posterior cingulate) was revealed in 7 patients including #13, mainly with focal or unilateral IEDs (see Fig. 6), corresponding to a notably higher proportion of cases than previously reported (Kobayashi et al., in press). No case of clear activation in the same region was found and the majority of these cases had very frequent IEDs or runs. The significance of this pattern is uncertain. The retrosplenial region has been implicated in fluctuations of cognition level (Gusnard et al., 2001) and shows changes in activity in relation to both the EEG alpha band and generalized spike-wave, and may represent downstream states changes linked to consciousness (Hamandi et al., in press). This is the subject of further investigation in our laboratory.

3.2.2. *The hemodynamic response to IEDs*

A high degree of variability in the shape of the HRF has been reported in normal subjects (Aguirre et al., 1998b). Based on our results, and in particular the high proportion of concordant activations, and from the data available to far (Benar et al., 2002; Krakow et al., 2001b; Lemieux et al., 2001), it would appear that IEDs primarily instigate physiological hemodynamic responses. Our data also suggest that negative responses tend to differ from the mirror image of the canonical (positive) HRF. Frequent events resulted in very small peak BOLD changes and in saturation (non-linear effects). The data are shown in Web Table 2.

3.2.3. *Clinical relevance*

The clinical relevance of EEG-fMRI rests on its ability to provide novel localizing information non-invasively and objectively in a good proportion of patients. This study demonstrates the technique's capability in patients with focal epilepsy and frequent IEDs.

In patients in whom electroclinical data already provides a likely generator, EEG-fMRI may provide some

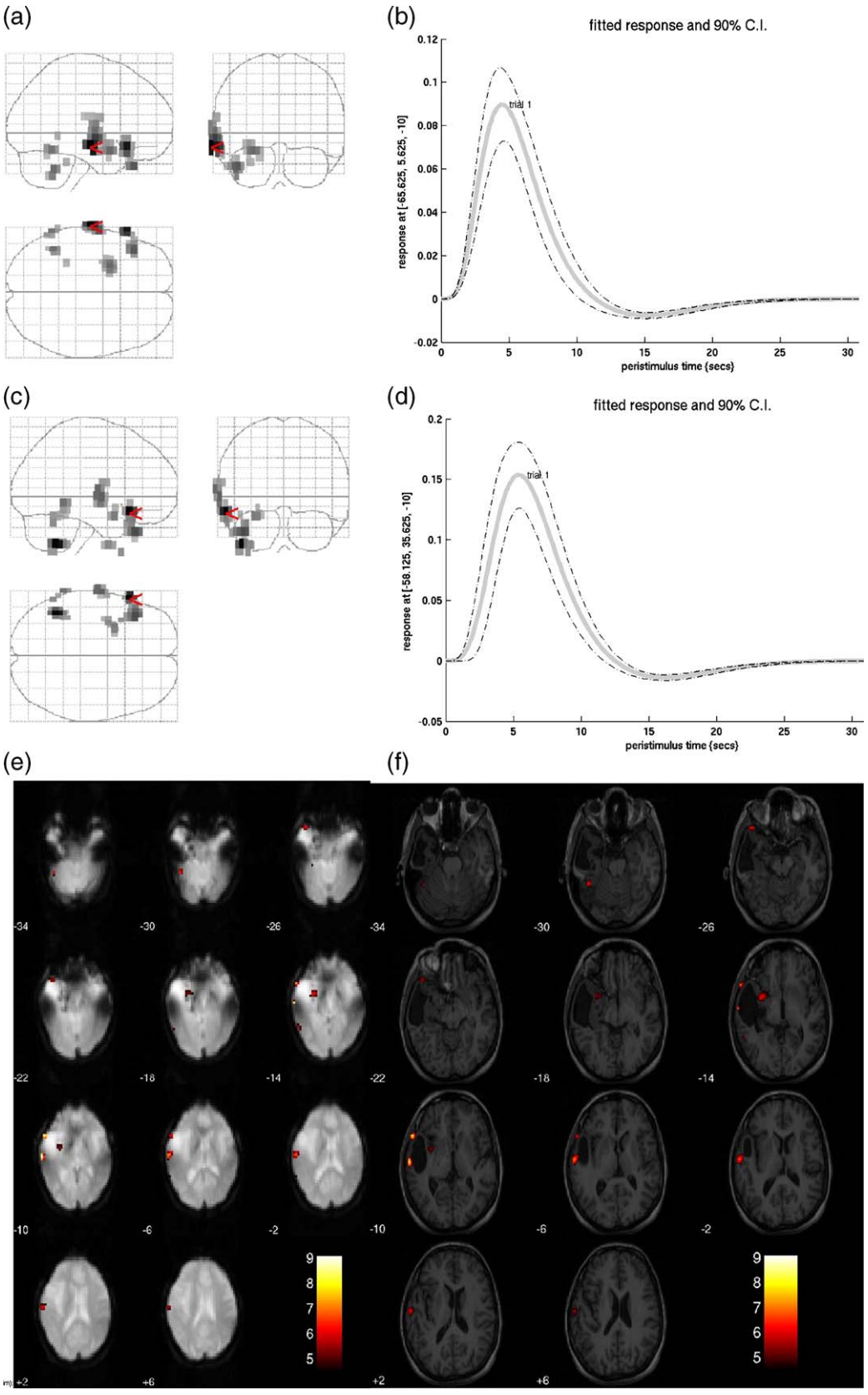

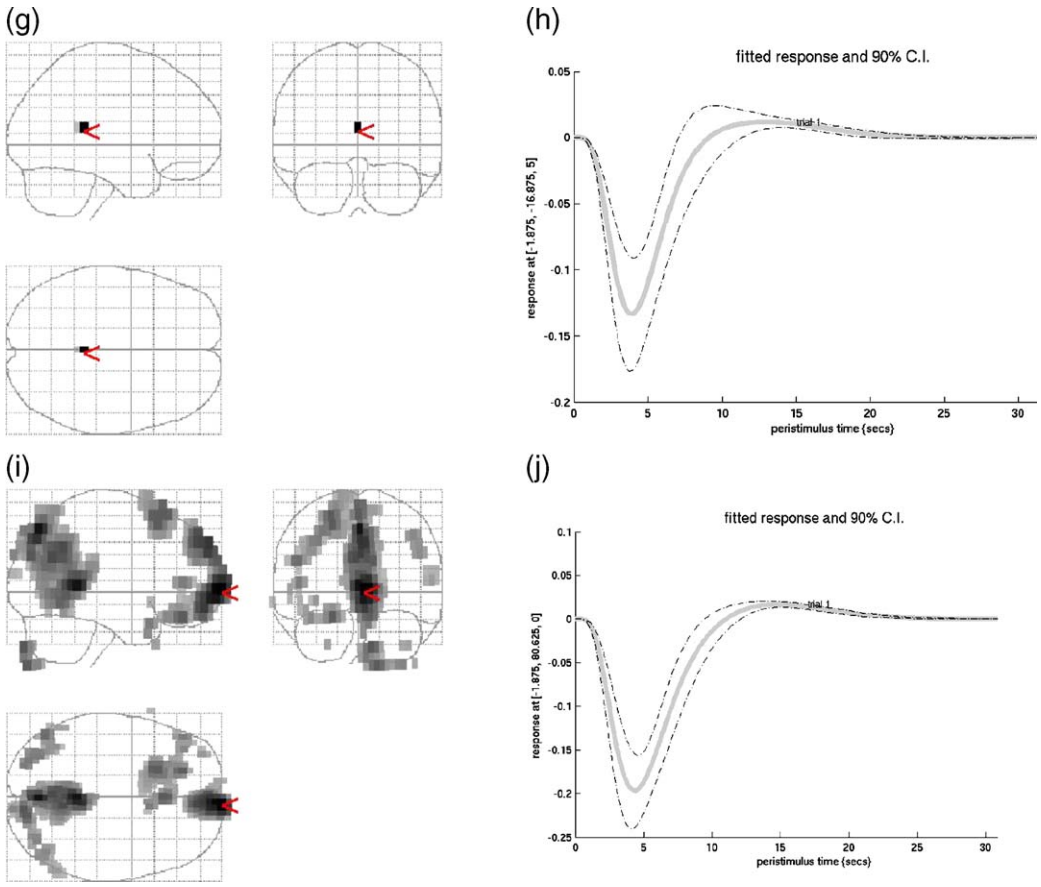

Fig. 5 – Concordant activation/Discordant deactivation. Patient #25 had left temporal lobe mass, probably neoplastic. During EEG/fMRI, there was continuous left anterior temporal spiking, shown in Fig. 1. Results are shown from two separate sessions, the first analyzed using a semi-automated spike-detection technique (a–b) and the second, conventionally (c–d). Spike-linked activation was exclusively seen around the cavity (a, c). The anatomical relationships are seen more clearly on the EPI (e) and T1 (f) overlays. There was minimal deactivation in the first session (g, h). During the second session, the patient was asked to open and close her eyes periodically, as it was discovered that the rate of spiking could be altered by doing so. The eyes closed/open condition was modeled separately as a confound. Spike-linked deactivations were marked during this session (i), (j).

degree of confirmation. The finding of localized activation in patients with poor electroclinical localization (#1, #4, #14, #18) is at least tantalizing in so far as indicating a potential role for EEG-fMRI to provide new hypotheses for testing, for example, as part of an implantation strategy for invasive EEG studies. A true interdisciplinary approach, however, remains essential to successfully carrying out such work in the clinical setting.

3.3. *Future work*

Higher density EEG allowing source modeling could enable the study of more subtle differences in IEDs and associated BOLD responses, especially at higher field strengths (Liston et al., in press-b). Physiological noise (cardiac, respiratory and background EEG rhythms) modeling also holds promise is this regard (Liston et al., in press-a). Clinically, future investigation needs focus on correlation/validation with invasive monitoring and surgical/pathological findings in specific syndromes to allow the direct testing of localization hypotheses derived from fMRI.

4. Experimental procedures

4.1. *Patients*

63 patients (25 males) who were attending the epilepsy clinics at either the National Hospital for Neurology and Neurosurgery, Queen Square, London, UK, or the National Society for Epilepsy (UK) with focal epilepsies were studied over a three year period. These patients were selected if they had frequent IEDs (spikes, polyspikes, sharp waves) on a recent EEG. The study was approved by the joint ethics committee of the National Hospital for Neurology and Neurosurgery and Institute of Neurology. Subjects gave informed, written consent.

In all patients, the seizure focus was first classified on the basis of the clinical, EEG, video-EEG telemetry and structural

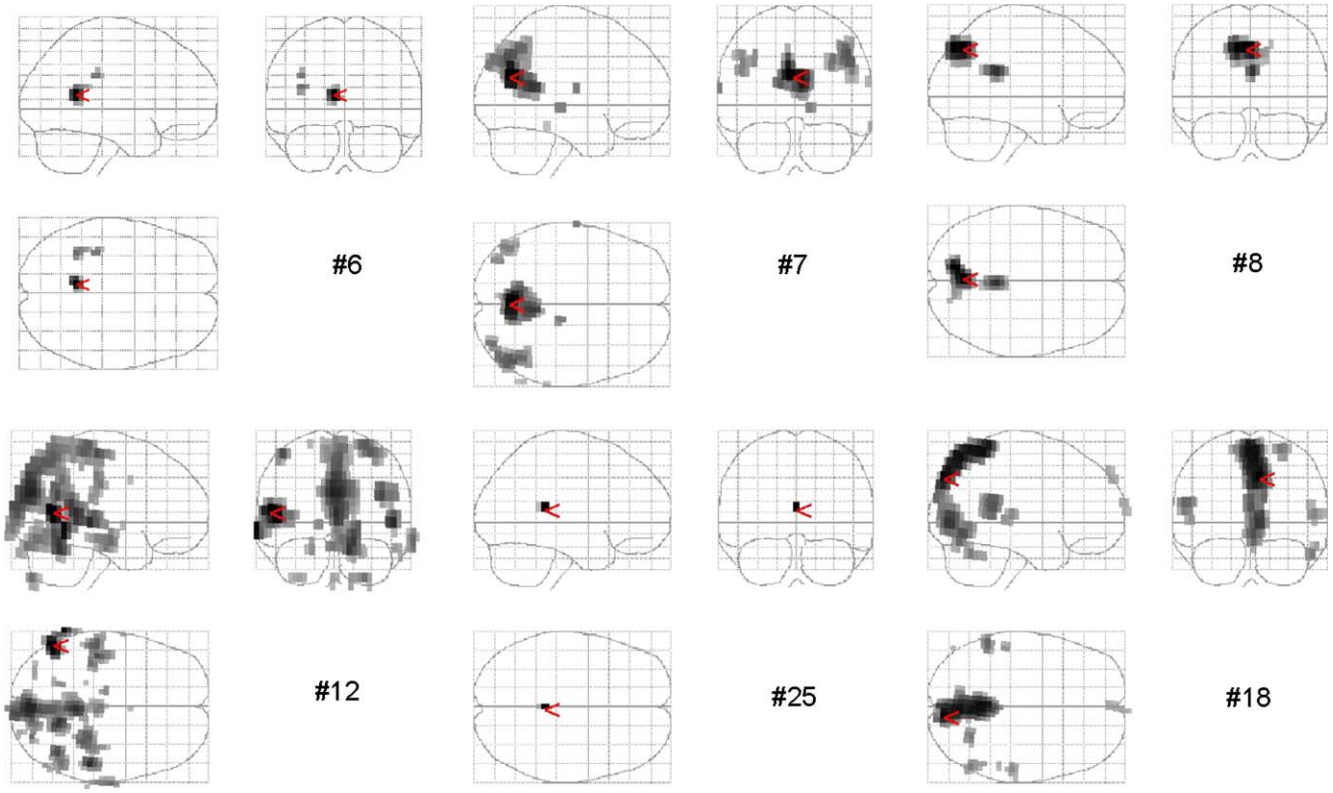

Fig. 6 – Pattern of bilateral medial occipital (precuneus) deactivation observed in 6 patients. SPM{-T} for negative HRFs, with the maximum indicated by red arrows. In case #12, the maximum is in the left parietal region, while in case #18, the maximum is in the posterior occipital region (sagittal sinus). See Fig. 3 for case #13. (For interpretation of the references to colour in this figure legend, the reader is referred to the web version of this article.)

MRI as being localized, lateralized or bifocal (e.g., bi-temporal), diffuse, multifocal or uncertain, by two of the authors (ASH and DRF) blind to the fMRI analysis.

4.2. *Data acquisition*

The patients were scanned on a 1.5 T Horizon EchoSpeed MRI scanner (General Electric, Milwaukee, USA) using T_2*-weighted single-shot gradient-echo echo-planar images (EPI; TE/TR 40/3000, flip angle: 90°, 21 × 5 mm interleaved slices, FOV = 24 × 24 cm, 64 × 64 matrix). 700 scans were acquired continuously over a 35-min period following an initial 12 s of scanning to achieve steady state magnetization. For the duration of the functional scans, patients were asked to keep their heads still and to keep their eyes shut. Standard manufacturer-supplied cushions, ear plugs and plastic ear defenders were used.

Twelve gold disk electrodes fitted with 10kOhm safety resistors were applied to the scalp, at Fp2/Fp1, F8/F7, T4/T3, T6/T7, O2/O1, Fz (ground) and Pz according to the international 10–20 system. Ten channels of EEG referenced to Pz and two channels of ECG were recorded as well was a timing signal derived from the scanner (5 kHz sampling, 33.3 mV range, 2 μV resolution) with online pulse (Allen et al., 1998) and imaging (Allen et al., 2000) artefact subtraction using MR-compatible equipment (Lemieux et al., 1997), providing good quality EEG display throughout the fMRI acquisition (see Fig. 1).

Table 3 – Experimental factors and presence of fMRI activation

Experimental factor	BOLD present (n = 23)	BOLD absent (n = 11)	Statistic
Head Motion (Mean ± SD)			
Mean |d'| (mm)	0.05 ± 0.04	0.09 ± 0.055	$P < 0.005^*$ (T)
Max |d'| (mm)	2.47 ± 5.57	23 ± 10.3	$P < 0.28$ (T)
Jerks	18.7 ± 30.2	54.9 ± 63.2	$P < 0.02$ (T)
IED characteristics			
Number (Mean ± SD)	355.2 ± 415.5	147.7 ± 269.1	$P < 0.12$ (T)
Runs/spikes (n = 8/31)	8/18	0/13	$P < 0.03^*$ (χ^2)
EEG background			
Mild/moderate/severe (n = 20/9/10)	18/5/3	2/4/7	$P < 0.004^*$ (χ^2)

4.3. *Pre-processing*

All fMRI data were analyzed using the SPM (Statistical Parametric Mapping) software package [http://www.fil.ion.ucl.ac.uk/spm/spm2.html]. and Matlab® version 6.5 R13 (The Mathworks Inc.,USA) running on a Dell® PowerEdge 2650 under Red Hat Linux 9. Images were slice-time corrected (Henson et al., 1999), realigned (Friston et al., 1995a), and

spatially smoothed using an isotropic Gaussian kernel of 8 mm FWHM. Scan realignment proceeds with an iterative estimation of the six rigid body motion parameters. In order to summarize the degree of head motion in each session, we estimated the absolute magnitude of the net displacement vector, *d*, using Pythagoras' theorem. The scan-to-scan displacement was calculated by estimating the absolute magnitude of the first derivative of d, $|d'|$. Individual head jerks were defined by $|d'| > 0.2$ mm/scan. These were counted automatically and incorporated into the fMRI model.

4.4. *EEG analysis*

Online EEG and ECG were used to monitor epileptiform activity, head motion, arousal level and eye movements. Offline EEG analysis and classification was carried out by 2 expert observers (ASH and BD or MM). EEG data were displayed in both referential and bipolar montages using in-house software. The classification objectives were: (1) to estimate the numbers and types of IED based on amplitude, spatial distribution and morphology; (2) to group events and onset times into different categories based on whether or not they were likely to share the same generators. Each event was marked manually using a mouse-driven time cursor to create a software-generated list of onset times, in relation to the fMRI data using scanner generated slice-timing information (Allen et al., 2000).

In five cases (#20, #25b, #29, #36, #39), a semi-automatic spike-detection method was used based on a threshold crossing algorithm. These were cases where unambiguous large-amplitude discharges were seen clearly against the background, with distinct phase reversal across 2 or more bipolar channels. But critically, occurring with such frequency so as to render manual identification impracticable (Salek-Haddadi et al., 2003). Firstly, any ambiguous or artefact contaminated segments of EEG were marked and excluded. A single compound EEG channel was then created by summing the two or more bipolar channels over which phase reversal takes place resulting in spikes being represented as large amplitude deflections. A threshold of two standard deviations was applied to the compound channel and all transition points, positive and negative, marked in time, along with the maximum amplitude of the detection channel between the transition points. A histogram of amplitude distribution was generated and the individual events at either extreme were recursively checked by visual inspection of the EEG and removed until the remaining band was free from artefacts. To exclude multiple events as part of the same IED complex, all events within one third of a second from the previous were removed.

4.5. *fMRI analysis*

For each patient, the analysis proceeded as follows:

4.5.1. *Step 1: Are there areas that display a conventional hemodynamic response to IEDs?*

To answer these, a mass-univariate approach was taken using the SPM2 implementation of the general linear model (GLM), to generate statistical parametric of the likelihood of an effect at each and every voxel (Friston et al., 1995b).

Design matrices (DMs) were assembled using sets of regressors spanning both the effects of interest and confounds. To protect against motion-related artefact, all design matrices included the six rigid-body motion correction parameters, $R_{i(i=1,\ldots,6)}(t)$, plus $R_i(t-1)$, $R_i(t)^2$ and $R_i(t-1)^2$. These can be regarded as confounding covariates corresponding to the first few terms of a Volterra series spanning the subspace of linear and non-linear motion-related effects (Friston et al., 1996). In addition, a number of scans were effectively removed from each session by modeling them explicitly within the DM as a single delta function. For every head jerk detected automatically (see above), a total of 4 scans were removed spanning a 12-s interval beginning with the jerk-scan. No subjects were therefore excluded specifically due to poor head motion. Both data and DM were high-pass filtered (1/200 s cutoff) and pre-whitened to remove slow drifts and correct for temporal non-sphericity (Friston et al., 2000).

IEDs were modeled through convolution of a series of delta functions specifying the EEG-derived onsets, with a canonical hemodynamic response function. A temporal derivative (orthogonal) was also included to account for small systematic differences in hemodynamic latency, as per the Taylor approximation (Friston et al., 1998a). A plain T-contrast, either positive or negative, was then used to test the relevant parameter estimate for statistical significance in relation to its standard error.

All results were thresholded at the $P<0.05$ level, corrected for multiple comparisons using Gaussian field theory (Friston et al., 1991). No cluster thresholds were applied and they were presented as Statistical Parametric Maps (SPMs), using the familiar glass-brain format to allow visualization of the entire activation pattern.

4.5.2. *Step 2: Are there areas that display any time-locked activity linked to IED, other than the above?*

The approach outlined in step 1 is potentially powerful but relies on the assumption that IED event-related responses are well approximated by a canonical HRF. We therefore looked for event-related responses of any form, when step 1 did not reveal activations. We used an event-locked Fourier basis set (8 sines and 8 cosines modulated with a Hanning filter) spanning a 45-s window to model the event-related response in an unconstrained fashion and tested for an effect using an F-test (Josephs et al., 1997).

4.5.3. *Step 3: Are the activated areas concordant with seizure focus?*

Where possible, we made categorical judgments regarding the fMRI concordance with the independently-determined focus. Activation patterns were classified as either *Concordant*, where the entire activation was concordant with the electroclinical localization; *Concordant plus* where maximum was concordant but additional, discordant clusters were seen; *Discordant*; or *Nil*, for no activation. This was done for both positive and negative BOLD responses.

When the focus was uncertain or diffuse, fMRI concordance was assessed in relation to the presumed generator of the interictal discharges.

4.5.4. *Step 4: What is the hemodynamic response to IEDs?*
Steps 4 and 5 were applied to patients with positive *Concordant* and *Concordant Plus* activations only. Event-related responses were estimated using SPM2 for both the most significant voxel and the most significant cluster as a whole. This was done by fitting a finite impulse response set (32×1 s bins) to the extracted timeseries and an eigentimeseries derived from singular value decomposition across the entire cluster, following filtering and adjustment for the effects of no interest. Each result was displayed as a peristimulus time histogram and summarized as a set of parameters (time to peak, time to undershoot, peak percentage change, and peak to undershoot ratio). The duration of each response was estimated visually.

4.5.5. *Step 5: Do IED characteristics influence the BOLD response?*

4.5.5.1. *A. Cases with multiple IED types.* In patients in whom more than one event type was recorded (#6, #25, #31, #35), we addressed two questions: firstly, which event types needed to be included in the model and secondly, whether any distinction among these event types was warranted. We used the principle of 'backward elimination' to select among a hierarchy of models (Draper and Smith, 1981). For example, where there were three event types corresponding to different IED amplitudes (#31 and #35), we compared three models representing different combinations of events: we began by combining all three as a single set of events: '1+2+3' (i.e., representing the assumption that all event types share the same generator) and tested for activations. The two other models were created and tested for activation by adding two different combinations of events: '1+2' (types 1 and 2 share the same generator) and '1' (type 1 events have their own generator). The same principle was used for the cases with 2 event types, giving: '1+2', '2'. Note that in our scheme, event types are ordered by presumed importance, i.e., type 1 represents the dominant IEDs, and other types represent types of decreasing importance. The differences in contribution of the various event types on the BOLD activation were assessed using F-tests.

4.5.5.2. *B. Cases with runs of IED.* In cases where runs/bursts of IEDs events were modeled using a single onset vector (#3, #7a, #13, #23a, and #23b), we explored the influence of the duration of the EEG run on the BOLD response. This was done using the concept of parametric modulation, to look for an effect on the amplitude of the BOLD (Buchel et al., 1998). We tested for additional variance explained using F-test.

4.5.5.3. *C. Cases with very frequent IED.* In cases with very frequent discharges (number >100 per 35-min scan, excluding runs) we looked for non-linear effects in the BOLD response, such as saturation (#6, #7b, #8, #9, #11, #12, #31, and #39. We used a Volterra expansion of the basis functions (Friston et al., 1998b). Here, we were only concerned with the presence or absence of such effects, for the global maxima.

Further details of the models and results for parts A, B and C are given in Web Table 1.

4.5.6. *What are the factors that influence the likelihood of activation?*
We examined quantitatively the link between activation and runs of IED versus single spikes, and the degree of abnormality of background rhythms (mild theta, moderate theta/delta, severe delta, loss of alpha or of other normal rhythms). The EEG background abnormalities were ranked visually as mild, moderate or severe for this purpose and the significance was assessed using the Chi-square statistic. We also looked for the effect of head motion as expressed by the mean and maximum scan-to-scan displacement and total number of spikes using two-sample *t*-tests to look for significant differences between the means in all patients with BOLD changes versus those without (BOLD vs. no-BOLD cases).

Acknowledgments

ASH was supported by the Medical Research Council (UK), and the University College London Hospitals NHS Trust. KH and LL are supported by the Wellcome Trust. The National Society for Epilepsy supports the MRI Unit. We thank the methods group at the Wellcome Department of Imaging Neuroscience, Institute of Neurology, UCL, for helpful discussions and Dr. H. Laufs for providing impetus.

Appendix A. Supplementary data

Supplementary data associated with this article can be found, in the online version, at doi:10.1016/j.brainres.2006.02.098.

REFERENCES

Aguirre, G.K., Zarahn, E., D'Esposito, M., 1998a. The inferential impact of global signal covariates in functional neuroimaging analyses. NeuroImage 8, 302–306.
Aguirre, G.K., Zarahn, E., D'Esposito, M., 1998b. The variability of human, BOLD hemodynamic responses. NeuroImage 8, 360–369.
Al Asmi, A., Benar, C.G., Gross, D.W., Khani, Y.A., Andermann, F., Pike, B., Dubeau, F., Gotman, J., 2003. fMRI activation in continuous and spike-triggered EEG-fMRI studies of epileptic spikes. Epilepsia 44, 1328–1339.
Allen, P.J., Polizzi, G., Krakow, K., Fish, D.R., Lemieux, L., 1998. Identification of EEG events in the MR scanner: the problem of pulse artifact and a method for its subtraction. NeuroImage 8, 229–239.
Allen, P.J., Josephs, O., Turner, R., 2000. A method for removing imaging artifact from continuous EEG recorded during functional MRI. NeuroImage 12, 230–239.
Archer, J.S., Briellman, R.S., Abbott, D.F., Syngeniotis, A., Wellard, R.M., Jackson, G.D., 2003. Benign epilepsy with centro-temporal

spikes: spike triggered fMRI shows somato-sensory cortex activity. Epilepsia 44, 200–204.
Bagshaw, A.P., Aghakhani, Y., Benar, C.G., Kobayashi, E., Hawco, C., Dubeau, F., Pike, G.B., Gotman, J., 2004. EEG-fMRI of focal epileptic spikes: analysis with multiple haemodynamic functions and comparison with gadolinium-enhanced MR angiograms. Hum. Brain Mapp. 22, 179–192.
Bagshaw, A.P., Hawco, C., Benar, C.G., Kobayashi, E., Aghakhani, Y., Dubeau, F., Pike, G.B., Gotman, J., 2005. Analysis of the EEG-fMRI response to prolonged bursts of interictal epileptiform activity. NeuroImage 24, 1099–1112.
Benar, C.G., Gross, D.W., Wang, Y., Petre, V., Pike, B., Dubeau, F., Gotman, J., 2002. The BOLD response to interictal epileptiform discharges. NeuroImage 17, 1182–1192.
Buchel, C., Holmes, A.P., Rees, G., Friston, K.J., 1998. Characterizing stimulus-response functions using nonlinear regressors in parametric fMRI experiments. NeuroImage 8, 140–148.
Diehl, B., Salek-Haddadi, A., Fish, D.R., Lemieux, L., 2003. Mapping of spikes, slow waves, and motor tasks in a patient with malformation of cortical development using simultaneous EEG and fMRI. Magn. Reson. Imaging 21, 1167–1173.
Draper, N.R., Smith, H., 1981. Applied Regression Analysis. Wiley, New York.
Engel Jr., J., 1993. Intracerebral recordings: organization of the human epileptogenic region. J. Clin. Neurophysiol. 10, 90–98.
Federico, P., Archer, J.S., Abbott, D.F., Jackson, G.D., 2005. Cortical/subcortical BOLD changes associated with epileptic discharges: an EEG-fMRI study at 3 T. Neurology 64, 1125–1130.
Fish, D.R., 2003. The role of scalp electroencephalography in presurgical evaluation. In: Shorvon, S.D., Fish, D.R., Dodson, E., Perucca, E., Olivier, A. (Eds.), The Treatment of Epilepsy. Blackwell, Oxford.
Friston, K.J., Frith, C.D., Liddle, P.F., Frackowiak, R.S., 1991. Comparing functional (PET) images: the assessment of significant change. J. Cereb. Blood Flow Metab. 11, 690–699.
Friston, K.J., Ashburner, J., Poline, J.B., Frith, C.D., Heather, J.D., Frackowiak, R.S., 1995a. Spatial registration and normalization of images. Hum. Brain Mapp. 2, 165–189.
Friston, K.J., Holmes, A.P., Worsley, K.J., Poline, J.B., Frith, C.D., Frackowiak, R.S., 1995b. Statistical parametric maps in functional imaging: a general linear approach. Hum. Brain Mapp. 2, 189–210.
Friston, K.J., Williams, S., Howard, R., Frackowiak, R.S., Turner, R., 1996. Movement-related effects in fMRI time-series. Magn. Reson. Med. 35, 346–355.
Friston, K.J., Fletcher, P., Josephs, O., Holmes, A., Rugg, M.D., Turner, R., 1998a. Event-related fMRI: characterizing differential responses. NeuroImage 7, 30–40.
Friston, K.J., Josephs, O., Rees, G., Turner, R., 1998b. Nonlinear event-related responses in fMRI. Magn. Reson. Med. 39, 41–52.
Friston, K.J., Josephs, O., Zarahn, E., Holmes, A.P., Rouquette, S., Poline, J., 2000. To smooth or not to smooth? Bias and efficiency in fMRI time-series analysis. NeuroImage 12, 196–208.
Gusnard, D.A., Raichle, M.E., Raichle, M.E., 2001. Searching for a baseline: functional imaging and the resting human brain. Nat. Rev., Neurosci. 2, 685–694.
Hamandi, K., Bagshaw, A., Laufs, H., Liston, A., Gotman, J., in press. Negative BOLD responses to epileptic spikes. NeuroImage.
Henson, R.N.A., Buchel, C., Josephs, O., Friston, K.J., 1999. The slice-timing problem in event-related fMRI. NeuroImage 9, 125.
Horsely, V., 1886. Brain surgery. Br. Med. J. 2, 670–675.
Jager, L., Werhahn, K.J., Hoffmann, A., Berthold, S., Scholz, V., Weber, J., Noachtar, S., Reiser, M., 2002. Focal epileptiform activity in the brain: detection with spike-related functional MR imaging preliminary results. Radiology 223, 860–869.
Josephs, O., Turner, R., Friston, K.J., 1997. Event-related fMRI. Hum. Brain Mapp. 5, 243–248.
Kobayashi, E., Bagshaw, A.P., Jansen, A., Andermann, F., Andermann, E., Gotman, J., Dubeau, F., 2005. Intrinsic epileptogenicity in polymicrogyric cortex suggested by EEG-fMRI BOLD responses. Neurology 64, 1263–1266.
Kobayashi, E., Bagshaw, A.P., Grova, C., Dubeau, F., Gotman, J., in press. Negative BOLD responses to epileptic spikes. Hum. Brain Mapp.
Krakow, K., Woermann, F.G., Symms, M.R., Allen, P.J., Lemieux, L., Barker, G.J., Duncan, J.S., Fish, D.R., 1999. EEG-triggered functional MRI of interictal epileptiform activity in patients with partial seizures. Brain 122 (Pt. 9), 1679–1688.
Krakow, K., Allen, P.J., Symms, M.R., Fish, D.R., Lemieux, L., 2001a. Imaging of interictal epileptiform discharges using spike-triggered fMRI. IJBME 1, 96–101.
Krakow, K., Lemieux, L., Messina, D., Scott, C.A., Symms, M.R., Duncan, J.S., Fish, D.R., 2001b. Spatio-temporal imaging of focal interictal epileptiform activity using EEG-triggered functional MRI. Epileptic Disord. 3, 67–74.
Lazeyras, F., Blanke, O., Perrig, S., Zimine, I., Golay, X., Delavelle, J., Michel, C.M., de Tribolet, N., Villemure, J.G., Seeck, M., 2000. EEG-triggered functional MRI in patients with pharmacoresistant epilepsy. J. Magn. Reson. Imaging 12, 177–185.
Lemieux, L., Allen, P.J., Franconi, F., Symms, M.R., Fish, D.R., 1997. Recording of EEG during fMRI experiments: patient safety. Magn. Reson. Med. 38, 943–952.
Lemieux, L., Salek-Haddadi, A., Josephs, O., Allen, P., Toms, N., Scott, C., Krakow, K., Turner, R., Fish, D.R., 2001. Event-related fMRI with simultaneous and continuous EEG: description of the method and initial case report. NeuroImage 14, 780–787.
Liston, A., Lund, T.E., Salek-Haddadi, A., Hamandi, K., Friston, K.J., Lemieux, L., in press-a. Modelling cardiac signal as a confound in EEG-fMRI and its application in focal epilepsy studies. NeuroImage.
Liston, A.D., De Munck, J.C., Hamandi, K., Laufs, H., Ossenblok, P., Duncan, J.S., Lemieux, L., in press-b. Analysis of EEG-fMRI data in focal epilepsy based on automated spike classification and signal space projection. NeuroImage.
Luders, H.O., Engel Jr., J., Munari, C., 1993. General principles. In: Engel Jr., J. (Ed.), Surgical Treatment of the Epilepsies. Raven Press, Ltd., New York, pp. 137–153.
Lund, T.E., Norgaard, M.D., Rostrup, E., Rowe, J.B., Paulson, O.B., 2005. Motion or activity: their role in intra- and inter-subject variation in fMRI. NeuroImage 26, 960–964.
Mauguiere, F., Ryvlin, P., 2004. The role of PET in presurgical assessment of partial epilepsies. Epileptic. Disord. 6, 193–215.
Patel, M.R., Blum, A., Pearlman, J.D., Yousuf, N., Ives, J.R., Saeteng, S., Schomer, D.L., Edelman, R.R., 1999. Echo-planar functional MR imaging of epilepsy with concurrent EEG monitoring. Am. J. Neuroradiol. 20, 1916–1919.
Plonsey, R., 1963. Reciprocity applied to volume conductors and the EEG. IEEE Trans. Biomed. Eng. 10, 9–12.
Rosenow, F., Luders, H., 2001. Presurgical evaluation of epilepsy. Brain 124, 1683–1700.
Salek-Haddadi, A., Merschhemke, M., Lemieux, L., Fish, D.R., 2002. Simultaneous EEG-correlated ictal fMRI. NeuroImage 16, 32–40.
Salek-Haddadi, A., Friston, K.J., Lemieux, L., Fish, D.R., 2003. Studying spontaneous EEG activity with fMRI. Brain Res. Rev. 43, 110–133.
Schomer, D.L., Bonmassar, G., Lazeyras, F., Seeck, M., Blum, A., Anami, K., Schwartz, D., Belliveau, J.W., Ives, J., 2000. EEG-Linked functional magnetic resonance imaging in epilepsy and cognitive neurophysiology. J. Clin. Neurophysiol. 17, 43–58.
Seeck, M., Lazeyras, F., Michel, C.M., Blanke, O., Gericke, C.A., Ives,

J., Delavelle, J., Golay, X., Haenggeli, C.A., de Tribolet, N., Landis, T., 1998. Non-invasive epileptic focus localization using EEG-triggered functional MRI and electromagnetic tomography. Electroencephalogr. Clin. Neurophysiol. 106, 508–512.

Symms, M.R., Allen, P.J., Woermann, F.G., Polizzi, G., Krakow, K., Barker, G.J., Fish, D.R., Duncan, J.S., 1999. Reproducible localization of interictal epileptiform discharges using EEG-triggered fMRI. Phys. Med. Biol. 44, N161–N168.

Warach, S., Ives, J.R., Schlaug, G., Patel, M.R., Darby, D.G., Thangaraj, V., Edelman, R.R., Schomer, D.L., 1996. EEG-triggered echo-planar functional MRI in epilepsy. Neurology 47, 89–93.